Original Article

Semiquantitative assessment of osteoblastic, osteolytic, and mixed lytic-sclerotic bone lesions on fluorodeoxyglucose positron emission tomography/computed tomography and bone scintigraphy

ABSTRACT

Bone scintigraphy is widely used to detect bone metastases, particularly osteoblastic ones, and F-18 fluorodeoxyglucose (FDG) positron emission tomography (PET) scan is useful in detecting lytic bone metastases. In routine studies, images are assessed visually. In this retrospective study, we aimed to assess the osteoblastic, osteolytic, and mixed lytic-sclerotic bone lesions semiquantitatively by measuring maximum standardized uptake value (SUV_{max}) on FDG PET/computed tomography (CT), maximum lesion to normal bone count ratio (ROI_{max}) on bone scintigraphy, and Hounsfield unit (HU) on CT. Bone scintigraphy and FDG PET/CT images of 33 patients with various solid tumors were evaluated. Osteoblastic, osteolytic, and mixed lesions were identified on CT and SUV_{max}, ROI_{max}, and HU values of these lesions were measured. Statistical analysis was performed to determine if there is a difference in SUV_{max}, ROI_{max}, and HU values of osteoblastic, osteolytic, and mixed lesions and any correlation between these values. Patients had various solid tumors, mainly lung, breast, and prostate cancers. There were 145 bone lesions (22.8% osteoblastic, 53.1% osteolytic, and 24.1% mixed) on CT. Osteoblastic lesions had a significantly higher value of CT HU as compared to osteolytic and mixed lesions ($P < 0.01$). There was no significant difference in mean ROI_{max} and mean SUV_{max} values of osteolytic and osteoblastic bone lesions. There was no correlation between SUV_{max} and ROI_{max}, SUV_{max} and HU, and ROI_{max} and HU values in osteolytic, osteoblastic, and mixed lesions ($P > 0.05$). Not finding a significant difference in SUV_{max} and ROI_{max} values of osteoblastic, osteolytic, and mixed lesions and also lack of correlation between SUV_{max}, ROI_{max}, and HU values could be due to treatment status of the bone lesions, size of the lesion, nonmetastatic lesions, erroneous measurement of SUV_{max} and ROI_{max}, or varying metabolism in bone metastases originating from various malignancies.

Keywords: Bone scintigraphy, fluorodeoxyglucose positron emission tomography/computed tomography, osteoblastic, osteolytic, semiquantitative

INTRODUCTION

Bone is one of the most common sites for metastatic spread of tumors. Tumors most commonly metastasizing to bone are prostate, breast, kidney, lung, and thyroid. In children, common causes of skeletal metastases include neuroblastoma, Ewing sarcoma, and osteosarcoma. In men, carcinoma of the prostate accounts for 60% of bone metastases, while in women, breast cancer accounts for 70% of such metastases. Metastases typically involve the axial skeleton, which is the region rich in red bone marrow. Bone metastases could be purely osteoblastic, mixed osteoblastic/osteolytic, or osteolytic. Prostate cancer metastases are purely osteoblastic, whereas metastases of thyroid and kidney carcinomas are

Guray Gurkan, Ismet Sarikaya[1], Ali Sarikaya[2]

Department of Nuclear Medicine, Sultan 1. Murat State Hospital, Kirklareli, [2]Department of Nuclear Medicine, Faculty of Medicine, Trakya University, Edirne, Turkey, [1]Department of Nuclear Medicine, Faculty of Medicine, Kuwait University, Kuwait City, Kuwait

Address for correspondence: Dr. Ismet Sarikaya, Department of Nuclear Medicine, Faculty of Medicine, Kuwait University, P.O. Box 24923, Safat 13110, Kuwait City, Kuwait. E-mail: isarikaya99@yahoo.com

How to cite this article: Gurkan G, Sarikaya I, Sarikaya A. Semiquantitative assessment of osteoblastic, osteolytic, and mixed lytic-sclerotic bone lesions on fluorodeoxyglucose positron emission tomography/computed tomography and bone scintigraphy. World J Nucl Med 2019;18:132-6.

purely lytic. Mixed osteolytic/osteoblastic lesions occur in carcinomas of the breast, lung, cervix, ovary, and testis.

Bone metastasis can be identified only when the distortion of the compact bone structure in the direct X-ray and computed tomography (CT) reach a certain level. Bone scintigraphy is the easiest and cheapest way to scan the whole body with a higher sensitivity than the specificity.[1-6] Whole body bone scan allows scanning the whole skeletal system. Single photon emission CT (SPECT), particularly SPECT/CT, further increases the sensitivity and specificity of bone scintigraphy for the detection of bone metastases. F-18 fluorodeoxyglucose (FDG) positron emission tomography/ CT (PET/CT) imaging is commonly used in oncology for staging of the tumors as well as detecting recurrences and assessing response to treatments. While bone scintigraphy assesses the osteoblastic activity of bone metastases, FDG PET scan evaluates the glucose metabolism/glycolysis of the lesions. Bone scintigraphy has higher sensitivity in detecting osteoblastic bone metastases than osteolytic ones.[7,8] In detecting osteolytic bone metastases, FDG PET/CT has been reported to be superior to bone scintigraphy.[3,4,7] Metastatic bone lesions can be detected in early stage on magnetic resonance imaging (MRI) with the signal changes in the bone marrow which is hypointense in suppressed T1 images and hyperintense in T2 images. Diffusion-weighted whole-body MRI was found to be equivalent to bone scintigraphy and FDG PET/CT in assessing bone metastases in non-small cell lung cancer.[9] There are various studies comparing FDG PET/CT with bone scintigraphy visually for the detection of bone metastases.[7,10-17] However, to the best of our knowledge, there is no study determining and comparing semiquantitative values of bone lesions on bone scintigraphy and FDG PET in patients with malignancies.

In this study, we aimed to determine semiquantitative measurement values of osteolytic, osteoblastic, and mixed-type bone lesions on bone scintigraphy and FDG PET/ CT images in patients with solid organ malignancies.

MATERIALS AND METHODS

Bone scintigraphy and F-18 FDG PET/CT images of patients with various solid tumors were selected for further analysis. This retrospective study was approved by the Ethics Committee of Trakya University Faculty of Medicine.

For bone scintigraphy, the patients were injected 20–25 mCi (740–925 MBq) technetium-99 m methylene diphosphonate, and images were obtained 2–4 h after the injection. Images included anterior and posterior whole body (10–15 cm/min

scan speed), and SPECT (64 images for 20–40 s each), and spot (500–1000 kct) images of the area of interest. Images were obtained at dual-head gamma camera (Siemens E. CAM, Erlangen, Germany and Philips BrightView, Milpitas, CA, USA) using low-energy high-resolution collimator with 120 keV energy settings and 20% window. 1024×512 matrix was used for whole body images and 64×64 matrix for SPECT. Images were evaluated visually and semiquantitatively. For semiquantitative analysis, a region of interest (ROI) was drawn over the bone lesion and normal bone to obtain maximum lesion to normal bone count ratio (ROI_{max}). JETStream Workspace version 3.0 was used for this semiquantitative analysis.

For FDG PET/CT study, the patients fasted 6 h before imaging. Blood glucose level was checked before FDG injection. The patients were given oral contrast1 h before the study. FDG was injected when the blood glucose level was <150 mg/dl. PET/ CT images were obtained at GE discovery 8 PET/CT camera (GE Medical Systems, Waukesha, USA) 60 min following intravenous injection of 296–555 MBq (8–15 mCi) F-18 FDG. Before PET image acquisition, a low-dose CT was obtained for attenuation correction and anatomic localization purposes. PET acquisition was 3 min/bed from top of the head to mid thighs. PET images were corrected for attenuation on the basis of the CT data and reconstructed using a standard iterative algorithm and reformatted into transaxial, coronal, and sagittal views. Maximum intensity projection images were also generated. Both attenuation corrected and non-corrected PET images as well as PET/CT fusion images were visually evaluated. Low-dose CT images were also assessed by a radiologist to determine osteoblastic, osteolytic, and mixed lesions which are consistent or suspicious for bone metastases. For semiquantitative analysis, maximum standardized uptake value (SUV_{max}), and Hounsfield unit (HU) values were measured from the lesions.

Number Cruncher Statistical System 2007 and PASS 2008 Statistical Software (Utah, USA) program were used for statistical analysis. Mann–Whitney U, Spearman's correlation coefficient, Pearson's Chi-squared, and Kruskal–Wallis tests were used.

RESULTS

A total of 33 patients were included in this study. Fifteen patients were female and 18 were male with an age range of 37–79 years (mean 60.09 ± 8.77). Patients had various solid tumors including lung cancer (42.4%), breast cancer (30.4%), prostate cancer (6.1%), and other (endometrial cancer, pancreatic cancer, malignant melanoma, parathyroid tumor,

renal cell carcinoma, soft-tissue sarcoma, and oral cavity tumor). There were 145 bone lesions (22.8% osteoblastic, 53.1% osteolytic, and 24.1% mixed osteoblastic-osteolytic metastases) on CT. Distribution of bone metastases included pelvis (24.1%), lower thoracic spine (17.9%), lumbar spine (16.6%), ribs and sternum (10.3%), lower limbs (9.7%), upper thoracic spine (7.6%), upper limbs (4.8%), and other regions (9%).

Mean SUV_{max} of osteolytic bone lesions (7.73 ± 4.35) was higher than mean SUV_{max} of osteoblastic (6.84 ± 3.03) and mixed (6.88 ± 3.10) lesions, but it was not statistically significant (0.876) [Tables 1 and 2].

Mean ROI_{max} of osteoblastic bone lesions (6.42 ± 4.22) was higher than mean ROI_{max} of osteolytic lesions (5.33 ± 3.60), but it was not statistically significant (0.077) [Tables 1 and 2]. Mean ROI_{max} of mixed metastases was 6.32 ± 4.03.

Mean HU SUV_{max} of osteoblastic bone lesions (344.09 ± 140.62) was higher than mean HU of osteolytic (233.39 ± 125.29) and mixed (254.86 ± 105.69) lesions and it was statistically significant ($P < 0.01$) [Tables 1 and 2].

In osteoblastic metastases, there was no correlation between SUV_{max} and ROI_{max}, SUV_{max} and HU, and ROI_{max} and HU values [Table 3].

In osteolytic metastases, there was no correlation between SUV_{max} and ROI_{max}, SUV_{max} and HU, and ROI_{max} and HU values [Table 3].

In mixed metastases, there was no correlation between SUV_{max} and ROI_{max}, SUV_{max} and HU, and ROI_{max} and HU values [Table 3].

DISCUSSION

Bone scintigraphy and FDG PET/CT imaging play an important role in the management of patients with malignancies. Bone scintigraphy images, whole body, spot, or SPECT, are usually assessed visually. Several studies have been published on semiquantitative analysis of bone scintigraphy. Erdi *et al*. developed a semiautomated image segmentation program to determine the total fraction of skeletal involvement with bone metastases.[18] Bone scan lesion area, bone scan lesion intensity, and bone scan lesion count were calculated from identified lesions to determine response to treatment.[19] Regional activity concentration of the injected tracer was measured on SPECT images.[20] In our study, we obtained maximum uptake ratio of bone lesion to normal bone to determine the degree of osteoblastic activity of the bone lesions.

SUV_{max} is a commonly used parameter on FDG PET/CT studies to assess the metabolic activity of the lesions which can help to differentiate benign from malignant lesion and determine the aggressiveness of the tumor. In a study by Cook *et al*., 81% of lytic bone metastases showed increased FDG uptake; however, only 40% of sclerotic bone lesions were detected on FDG PET.[21] Abe *et al*. found that FDG PET was superior to bone scintigraphy in detecting osteolytic metastases, while bone scintigraphy was superior to FDG PET in detecting osteoblastic lesions.[12] In a study by Hur *et al*., SUV_{max} was significantly higher in osteolytic metastasis than in osteoblastic lesions.[16] Cook *et al*. found that the FDG uptake of osteoblastic metastases (mean SUV_{max}: 0.95) was significantly lower than the FDG uptake of osteolytic metastases (mean SUV_{max}: 6.77).[21]

As opposed to literature, in our study, we did not find a significant difference in mean SUV_{max} and ROI_{max} values of osteoblastic, osteolytic, and mixed lesions and there was also no correlation between the SUV_{max}, ROI_{max}, and HU values. Various factors may alter the mean SUV_{max} and ROI_{max} values. In our cases, some of the lesions seen on CT could be active metastatic disease and some inactive. For example, some of the sclerotic lesions on CT could be active osteoblastic metastases and some could be treated old lesions. Increased uptake on bone scan in a sclerotic lesion could be due to flare phenomenon in a treated osteoblastic, osteolytic, or mixed metastases.[22] Lack of increased activity on bone scan in a sclerotic lesion may be due to treated very old osteoblastic

Table 1: Kruskal-Wallis test comparing mean maximum standardized uptake value, region of interest, and hounsfiled unit values in osteoblastic, osteolytic and mixed lesions

| | Metastaz tipi | | | P |
| | Osteoblastic | Osteolytic | Mixed | |
	Mean±SD (median)	Mean±SD (median)	Mean±SD (median)	
PET SUV_{max}	6.84±3.03 (6)	7.73±4.35 (6.3)	6.88±3.10 (5.9)	0.876
Bone ROI_{max}	6.42±4.22 (5.2)	5.33±3.60 (4.2)	6.32±4.03 (5.1)	0.077
CT HU	344.09±140.62 (347)	233.39±125.29 (203)	254.86±105.69 (222)	0.001**

**: Significant, $P<0.01$; HU: Hounsfiled unit; SUV_{max}: Maximum standardized uptake value; PET: Positron emission tomography; CT: Computed tomography; ROI_{max}: Maximum region of interest; SD: Standard deviation

Table 2: *Post hoc* Mann-Whitney U-test results

	Osteoblastic/ osteolytic (*P*)	Osteoblastic/ mixed (*P*)	Osteolytic/ mixed (*P*)
PET SUV$_{max}$	0.737	0.893	0.638
Bone ROI$_{max}$	0.098	0.995	0.053
CT HU	0.001**	0.003**	0.155

**: Significant, $P<0.01$; HU: Hounsfiled unit; SUV$_{max}$: Maximum standardized uptake value; PET: Positron emission tomography; CT: Computed tomography; ROI$_{max}$: Maximum region of interest

Table 3: Spearman's rho correlation analysis results in between Maximum standardized uptake value, Maximum region of interest, and hounsfiled unit values

	PET SUV$_{max}$/ bone ROImax	PET SUV$_{max}$/ CT HU	BoneROI$_{max}$/ CT HU
Osteoblastic			
r	0.107	0.064	0.075
P	0.552	0.723	0.679
Osteolytic			
r	−0.194	0.159	−0.216
P	0.091	0.167	0.060
Mixed			
r	−0.160	−0.180	0.086
P	0.359	0.301	0.623

HU: Hounsfiled unit; SUV$_{max}$: Maximum standardized uptake value; PET: Positron emission tomography; CT: Computed tomography; ROI$_{max}$: Maximum region of interest
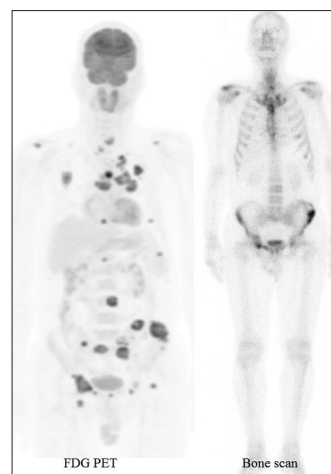

Figure 1: Fluorodeoxyglucose positron emission tomography/computed tomography maximum intensity projection image and bone scan in a patient with non-small cell lung cancer. Fluorodeoxyglucose positron emission tomography demonstrates multiple bone and lymph node metastases in addition to primary tumor in the left lung. Bone scan demonstrates metastasis in the left iliac bone and right acetabulum and superior pubic ramus. Computed tomography, not shown here, demonstrated multiple osteolytic bone metastases. Note that bone scan shows cold and hot pattern in the left iliac lytic lesion. There is also mildly increased uptake in right distal clavicle, sternum, and few left anterior ribs

metastasis. Sclerotic changes on CT in a treated bone metastasis may last longer than osteoblastic activity on bone scan. Increased uptake on bone scan due to flare is usually not seen on follow-up bone scan at 6 mos.[23] Flare phenomenon in bone metastases has also been reported with FDG PET/CT study.[24] Development of fracture in a lytic lesion may cause increased uptake on bone scan. Some sclerotic, lytic, or mixed lesions on CT may not be metastatic and could be due to various benign pathologies such as cyst or hemangioma. Measurement of SUV$_{max}$ is also affected by various factors such as blood glucose level at the time of injection, duration of the uptake period, body weight, and body composition. SUV$_{max}$ may be overestimated in sclerotic lesions due to over attenuation correction by CT, and it may be underestimated in osteolytic lesions due to under attenuation correction by CT. In small lesions, partial volume averaging may cause erroneous results for bone scintigraphy and FDG PET scan. For example, uptake of a small osteolytic lesion on bone scintigraphy may be overestimated and uptake of a small osteoblastic lesion may be underestimated. ROI$_{max}$ value of bone lesion is affected by underlying normal bone uptake on planar imaging. SPECT or SPECT/CT may provide more accurate ROI$_{max}$ values. Lytic lesions, particularly large ones, are not always seen cold on bone scan as seen in Figure 1 which can further increase mean value of the ROI$_{max}$. Our study consisted of various malignancies. Metabolic behavior of the osteoblastic and osteolytic bone lesions may vary in malignancies.

CONCLUSION

We did not find a significant difference in SUV$_{max}$ and ROI$_{max}$ values of osteoblastic, osteolytic, and mixed lesions and also lack of correlation between SUV$_{max}$, ROI$_{max}$, and HU values which could be due to various technical or patient-related causes or varying metabolism of bone metastases from various malignancies. A study with a larger number of patients who had untreated and proven bone metastases and also using SPECT instead planar bone imaging can be valuable to assess the metabolic and osteoblastic activities of bone metastases.

Conflicts of interest
There are no conflicts of interest.

REFERENCES

1. Messiou C, Cook G, deSouza NM. Imaging metastatic bone disease from carcinoma of the prostate. Br J Cancer 2009;101:1225-32.
2. Bares R. Skeletal scintigraphy in breast cancer management. Q J Nucl Med 1998;42:43-8.
3. Cook GJ, Fogelman I. Skeletal metastases from breast cancer: Imaging with nuclear medicine. Semin Nucl Med 1999;29:69-79.
4. Cook GJ, Fogelman I. The role of nuclear medicine in monitoring treatment in skeletal malignancy. Semin Nucl Med 2001;31:206-11.
5. Ell PJ. Skeletal imaging in metastatic disease. Curr Opin Radiol 1991;3:791-6.

6. Dotan ZA. Bone imaging in prostate cancer. Nat Clin Pract Urol 2008;5:434-44.

7. Zhang L, Chen L, Xie Q, Zhang Y, Cheng L, Li H, *et al.* A comparative study of 18F-fluorodeoxyglucose positron emission tomography/computed tomography and (99m)Tc-MDP whole-body bone scanning for imaging osteolytic bone metastases. BMC Med Imaging 2015;15:7.

8. Woolfenden JM, Pitt MJ, Durie BG, Moon TE. Comparison of bone scintigraphy and radiography in multiple myeloma. Radiology 1980;134:723-8.

9. Takenaka D, Ohno Y, Matsumoto K, Aoyama N, Onishi Y, Koyama H, *et al.* Detection of bone metastases in non-small cell lung cancer patients: Comparison of whole-body diffusion-weighted imaging (DWI), whole-body MR imaging without and with DWI, whole-body FDG-PET/CT, and bone scintigraphy. J Magn Reson Imaging 2009;30:298-308.

10. Rodrigues M, Stark H, Rendl G, Rettenbacher L, Datz L, Studnicka M, *et al.* Diagnostic performance of [18F] FDG PET-CT compared to bone scintigraphy for the detection of bone metastases in lung cancer patients. Q J Nucl Med Mol Imaging 2016;60:62-8.

11. Yang SN, Liang JA, Lin FJ, Kao CH, Lin CC, Lee CC, *et al.* Comparing whole body (18)F-2-deoxyglucose positron emission tomography and technetium-99m methylene diphosphonate bone scan to detect bone metastases in patients with breast cancer. J Cancer Res Clin Oncol 2002;128:325-8.

12. Abe K, Sasaki M, Kuwabara Y, Koga H, Baba S, Hayashi K, *et al.* Comparison of 18FDG-PET with 99mTc-HMDP scintigraphy for the detection of bone metastases in patients with breast cancer. Ann Nucl Med 2005;19:573-9.

13. Liu FY, Chang JT, Wang HM, Liao CT, Kang CJ, Ng SH, *et al.* [18F] fluorodeoxyglucose positron emission tomography is more sensitive than skeletal scintigraphy for detecting bone metastasis in endemic nasopharyngeal carcinoma at initial staging. J Clin Oncol 2006;24:599-604.

14. Fujimoto R, Higashi T, Nakamoto Y, Hara T, Lyshchik A, Ishizu K, *et al.* Diagnostic accuracy of bone metastases detection in cancer patients: Comparison between bone scintigraphy and whole-body FDG-PET. Ann Nucl Med 2006;20:399-408.

15. Shreve PD, Grossman HB, Gross MD, Wahl RL. Metastatic prostate cancer: Initial findings of PET with 2-deoxy-2-[F-18]fluoro-D-glucose. Radiology 1996;199:751-6.

16. Hur J, Yoon CS, Ryu YH, Yun MJ, Suh JS. Accuracy of fluorodeoxyglucose-positron emission tomography for diagnosis of single bone metastasis: Comparison with bone scintigraphy. J Comput Assist Tomogr 2007;31:812-9.

17. Ito S, Kato K, Ikeda M, Iwano S, Makino N, Tadokoro M, *et al.* Comparison of 18F-FDG PET and bone scintigraphy in detection of bone metastases of thyroid cancer. J Nucl Med 2007;48:889-95.

18. Erdi YE, Humm JL, Imbriaco M, Yeung H, Larson SM. Quantitative bone metastases analysis based on image segmentation. J Nucl Med 1997;38:1401-6.

19. Brown MS, Chu GH, Kim HJ, Allen-Auerbach M, Poon C, Bridges J, *et al.* Computer-aided quantitative bone scan assessment of prostate cancer treatment response. Nucl Med Commun 2012;33:384-94.

20. Cachovan M, Vija AH, Hornegger J, Kuwert T. Quantification of 99mTc-DPD concentration in the lumbar spine with SPECT/CT. EJNMMI Res 2013;3:45.

21. Cook GJ, Houston S, Rubens R, Maisey MN, Fogelman I. Detection of bone metastases in breast cancer by 18FDG PET: Differing metabolic activity in osteoblastic and osteolytic lesions. J Clin Oncol 1998;16:3375-9.

22. Janicek MJ, Hayes DF, Kaplan WD. Healing flare in skeletal metastases from breast cancer. Radiology 1994;192:201-4.

23. Coleman RE, Mashiter G, Whitaker KB, Moss DW, Rubens RD, Fogelman I, *et al.* Bone scan flare predicts successful systemic therapy for bone metastases. J Nucl Med 1988;29:1354-9.

24. Krupitskaya Y, Eslamy HK, Nguyen DD, Kumar A, Wakelee HA. Osteoblastic bone flare on F18-FDG PET in non-small cell lung cancer (NSCLC) patients receiving bevacizumab in addition to standard chemotherapy. J Thorac Oncol 2009;4:429-31.